The Korean Journal of Ceramics, **5** [1] 19 - 24 (1999)

Mechanical Properties and Electrical Discharge Machinability of β-Sialon-TiB_2 Composites

Yong-Kap Park, Jun-Tae Kim and Yong-Hyuck Baik*

Division of Metallurgical & Materials Engineering, Sunmoon University
**Department of Ceramic Engineering, Chonnam National University*
(Received January 15, 1999)

The influences of TiB_2 additions to the β-sialon on mechanical properties and electrical discharge machinability were investigated. Samples were prepared by adding 15, 30 and 45 vol.% TiB_2 particles as a second phase to a β-sialon matrix. The β-sialon-TiB_2 composites were sintered by hot pressing in a nitrogen atmosphere at 1800°C with pressure of 30 MPa. The fracture toughness of the composites was increased with the TiB_2 content except 45 vol.% TiB_2 composite. The crack propagation and crack deflection were observed with a SEM for etched samples after vicker's indentation. The composites containing more than 30 vol.% TiB_2 had resistivity lower than 10^{-3} Ωcm. The electrical discharge machining (EDM) of composites was conducted with two kind of machines such as die-sinker and wire cutter. The machinability was evaluated with the cutting rate and surface roughness after machining.

Key words : β-Sialon, Sialon-TiB_2 composites, Crack deflection, Electrical resistivity, Electrical discharge machining

I. Introduction

β-Sialon ceramics as one of the high temperature structural materials consist of Si_3N_4 solid solution with several oxides like Al_2O_3 and the solid solution is denoted $Si_{6-z}Al_zO_zN_{8-z}$, where $0<z\leqq 4.2$.[1-5] These ceramics together SiC, Si_3N_4 are applicable to industrial components such as mechanical seal, cutting tools and wear components instead of metals due to superior characteristics as their high thermal resistance, high wear resistance and high temperature strength. The material, however, still has problems to use as structural ceramics because of low fracture toughness, poor sinterability and poor machinability. One of the most difficult points to fabricate is poor machinability of extremely hard ceramic materials, because the sintered ceramics must be usually machined to get the designed shape. The poor machinability also increases processing cost and restricts the fabrication of complicated shapes. Therefore, the machining methods of structural ceramics need to be improved to expend their applications. The electrical discharge machining (EDM) is recently used to improve the machinability of the structural ceramics. The electrical discharge machining is especially effective for machining of complicate shapes which are impossible to be machined by conventional machining methods. The ceramic material should be electrically conductive to preform the electrical discharge machining. In case of electrical insulating ceramic materials, conductive particles such as metal compounds (ie., borides TiB_2, ZrB_2, carbides TiC and nitrides TiN) is usually reinforced to ceramic material.[6-10] In the last few years, several studies for the electrical discharge machining(EDM) have been done to improve the machinability of electrical conductive material reinforced SiC, Si_3N_4 and alumina based composites.[11-18] In the present study, TiB_2 particles have been added to sialon to enhance their electrical conductivity. Hence, the objectives of this study are to fabricate β-sialon-TiB_2 composites and evaluate their mechanical properties and electrical discharge machinability.

II. Experimental procedure

Si_3N_4, AlN, Y_2O_3 (H. C Starck, Germany) and Al_2O_3(AES-IIC, Sumitomo, Japan) powders were used in this study. The characteristics of the starting powers are shown in Table 1. The general formula of β-sialon are described as follows, where $0<Z<4$

$$(6\text{-}Z)Si_3N_4+ZAl_2O_3+ZAlN \rightarrow 3Si_{6-Z}Al_ZO_ZN_{8-Z} \quad (1)$$

Table 1. Characteristics of Starting Powders

	Impurities(wt.%)				Mean particle size (μm)
Si_3N_4	N	38.88	Fe	13 ppm	0.7 μm
	C	0.15	Al	490 ppm	
	O	1.20	Ca	55 ppm	
AlN	N	33%	C	600 ppm	3.85 μm
	O	1.05	Fe	230 ppm	
Al_2O_3	H_2O	0.12	Fe_2O_3	0.01	0.4 μm
	L.I.O	0.05	Na_2O	0.04	
	SiO_2	0.06	MgO	0.03	
Y_2O_3	O	0	0.14		0.7 μm
TiB_2	Free B	28.5	N	0.25	3.5 μm
	C	0.25	Fe_{Met}	0.1	
	O	2.0			

Table 2. Conditions of Wire and Die-sink EDM

EDM	Tool Electrodes	Dia. of Electrodes (μs)	Pulse Interval τ on (on-time) (μs)	Pulse Interval τoff (off-time) (μs)	Voltage (V)	Electric Current Peak intensity (Ip, A)	Condenser capacity (μF)	Width of Sample (mm)
Wire EDM	Cu+Zn (30%)	0.25	1.4~0.25	8	70~50	7~3	0.15	5
Die-sink EDM	Cu, (first machining)	15	50	75	50	5	-	
	Cu, (second machining)	15	6	9	50	3	-	

The Z value in the formular is taken as 0.5 in present work. The composition was 86 wt.% Si_3N_4, 5.6 wt.% Al_2O_3, 2.4 wt.% AlN and 6 wt.% Y_2O_3 as sintering aid. The amounts of TiB_2 added to the sialon composition were 15 vol.%, 30 vol.% and 45 vol.%. The four powder batches were prepared and milled in isoprophyl alcohol in a polyurethane ball mill jar with Si_3N_4 grinding media for 24 h. After milling, the mixtures were dried and sieved through a 200 mesh screen (-75 μm) to remove the agglomates. The dried powders were hot-pressed under the pressure of 30 MPa for 1h in a nitrogen atmosphere at 1800°C to obtain rectangular samples of 65 mm×75 mm and 5 mm in thickness. The sintered densities were determined by Archimedes principle. For the composites, the values were calculated with the rule of mixtures assuming that no reaction takes place between sialon matrix and the second phase. Phase identification and microstructural observation of fracture surfaces were carried out with a X-ray diffrectometer (philips, U.S.A.) and a scanning electron microscope (JSM-840A, Jeol, Japan). Polished surfaces were etched with a boiled NaOH solution in 30 sec to observe the average grain size and second phase(TiB_2) of the matrix. The flexural strengths were measured on samples 3 mm×4 mm×35 mm in three point bending machine, outer span 30 mm, with a cross head speed of 0.5 mm/min. Test bars were cut from sintered samples and ground to size with edges chamfered prior to testing. Microhardness was determined by indentation method with Vicker's microhardness tester (matsuzawa. model DVK-2S, Japan). The applied load, speed and holding time were 10 kgf, 40 μm/sec and 10 sec, respectively. Average values obtained after measuring 10 pieces were selected in this study. After measuring the microhardness of sintered sample, fracture behaviour was observed by a scanning electron microscope. The electrical resistivities of the sialon-TiB_2 composites were measured by a 4-point probe method (sheet resistivity 5 mΩ/sq-500 kΩ/sq Model CMT-SR 1000). The size of test samples was 30 mm ×40 mm×5 mm thickness. Electrical discharge machining(EDM) was carried out 15, 30 and 45 vol.% TiB_2 composites through wire(Model JAPAX LDM-50) and die-sinking EDM(MECCA, Ehwa, co.). Wire EDM uses a thin metallic wire like a jigsaw whose quality consist of copper and zinc(30%). In wire EDM, water is usually used as the dielectric. Wire is anode and workpiece is cathode. In die-sinkers used kerosene as dielectric solution, the workpiece and tool are cathode and anode, respectively. The anode is copper with 15 mm in diameter. In the present work, EDM test were carried out 30 vol.% and 45 vol.% TiB_2 composites through wire-EDM and die-sink EDM. The cutting rate and surface roughness of workpiece were evaluated as the characterization of EDM in this study. The specimen was retangular size of 65 mm×75 mm with 5 mm thick, which was machined by a wire-EDM and a die-sink EDM. After EDM, the machined surfaces also were examined by scanning electron microscope (SEM). The conditions of EDM showed in the Table 2.

III. Results and discussion

1. Phase analysis

Fig. 1 shows X-ray diffraction pattern of sialon and its composites which are formed by adding 15, 30 and 45 vol% TiB_2 to sialon. The main peaks came from β-sialon. The peak intensity decreases with increasing the amount of TiB_2. Compounds such as mellinite($Si_3N_4 \cdot Y_2O_3$) and yttrium aluminum oxide($YAlO_3$) were not detected, which are expected to be formed by the reaction among sintering

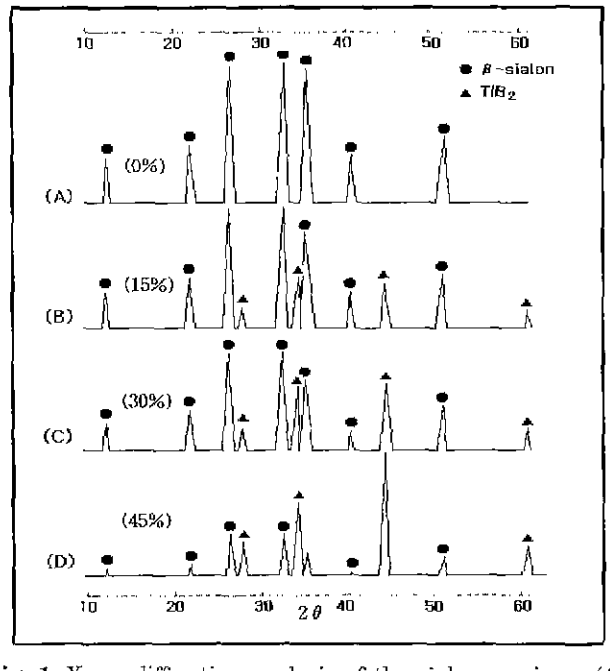

Fig. 1. X-ray diffraction analysis of the sialon specimen (A) and sialon-TiB_2 specimens (B, C, D).

aid(Y_2O_3) and composition of sialon(Si_3N_4 and Al_2O_3).[10] This might be attributed to the reason that these compounds exist as liquid phase along grain boundaries. A possible reaction during sintering process is considered as following;

$$5.5Si_3N_4+0.5AlN+0.5Al_2O_3(+Y_2O_3) \rightarrow 3Si_{6.5}Al_{0.5}O_{0.5}N_{7.5} \text{ (+grain boundary phase)} \quad (2)$$

TiB_2 particles exist inside sialon as second phase. It was not detected that the TiB_2 particles react with compounds which form sialon.

2. Densification and microstructure

The samples of monolithic sialon and composites containing 15~30 vol.% TiB_2 showed good densification above 99%, however, the composite with 45 vol% of TiB_2 showed 98% of the theoretical density. The sintered densities of monolithic sialon and 15, 30 and 45vol% TiB_2 composites were 3.16 g/cm^3, 3.34 g/cm^3, 3.54 g/cm^3 and 3.71 g/cm^3, respectively. The increase of TiB_2 content decrease the relative density value. It seems that the decrease of density cause the poor sinterability and the agglomation of TiB_2 particles. Fig. 2 is SEM micrographs of the fracture surface (a) and etched surface (b) of the sialon sample.

Fig. 3 shows microstructure of β-sialon-30 vol.% TiB_2 composite. In the micrographs, the plate-like grains or rod-like grains were β-sialon and large quasi-spherical grains were TiB_2. The sialon shows also elongated rod-like grain. As shown in Fig. 3, the TiB_2 particles are randomly distributed in the sialon matrix. Fig. 3(b) is the micrograph of sialon-30 vol% TiB_2 composites which prepared by chemical etching, where the pores and voids result from the detachment of TiB_2 particles and disolution of grain boundary by echant. The micrographs except 45 vol.% TiB_2 composite showed densified morphologies having homogeneous dispersed TiB_2 grains. Most TiB_2 particles are separated grains, but some clusters of several grains are also observed. This may occur because of the difficulty in dispersing TiB_2 single particle as the TiB_2 content is increased. The micrographs show that TiB_2 particles impede the grain growth of sialon, especially, the discontinuous grain growth. Hence, monolithic grain reveal the duplex microstructure, which formed the elongated and exaggerated grain due to abnormal grain growth. The TiB_2 particles, however, inhibit the exaggerated grain growth of sialon grain which result in rather homogeneous microstructures. It seems that the TiB_2 particles did not help the grain growth of sialon occurring during densification.

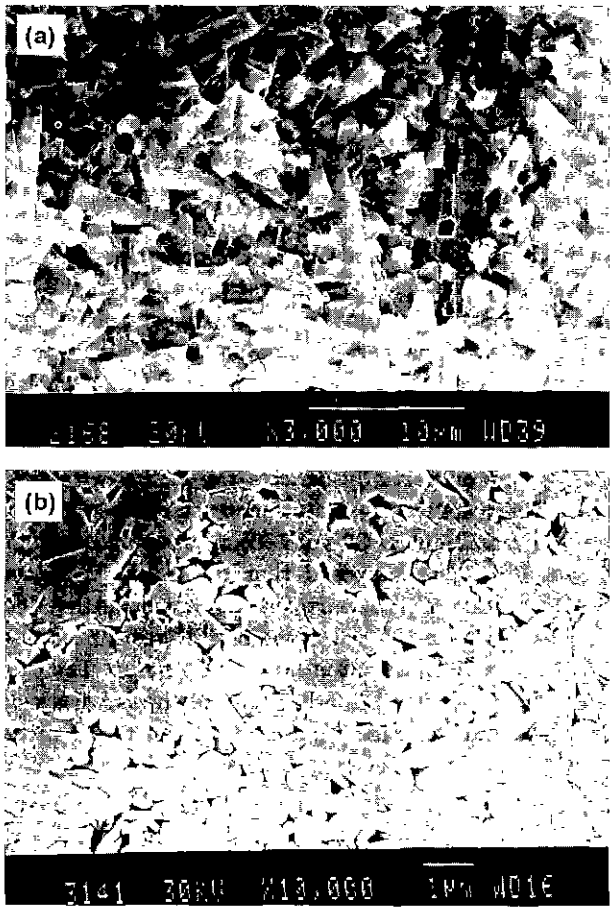

Fig. 2. SEM micrographs of the fracture surface (a) and etched surface (b) of the sialon sample.

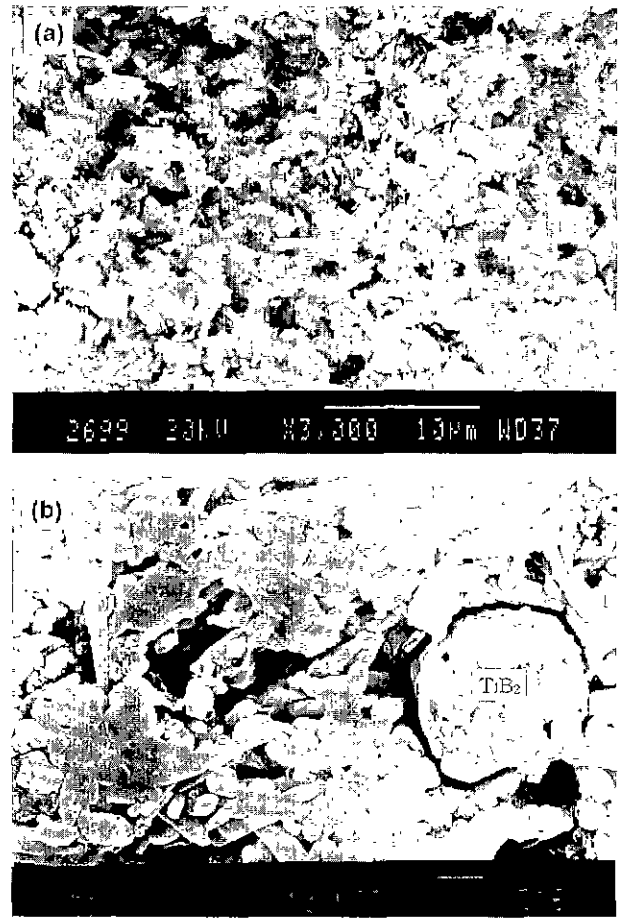

Fig. 3. SEM micrographs of the fracture surface (a) and etched surface (b) of the sialon-30 vol.% TiB_2 sample.

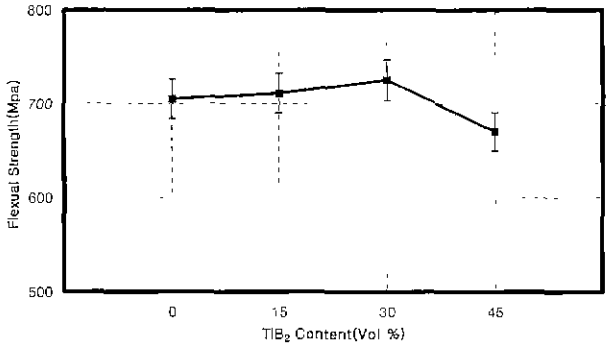

Fig. 4. Flexural strength of sialon and sialon composites as a function of TiB_2 content.

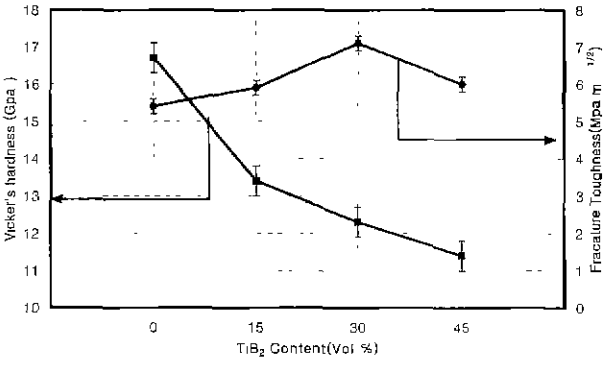

Fig. 5. Hardness and fracture toughness of sialon composites as a function of TiB_2 content.

It was considered that TiB_2 particles occupied the space growing the grain growth and impeded the solution-reprecipitation in need of grain growth.

3. Mechanical properties

Fig. 4, 5 show flexural strength, microhardness and fracture toughness of monolithic sialon and sialon-TiB_2 composites. The flexural strength values slightly increased with TiB_2 content, while that of the 45 vol.% composite decreased. The strength decrease seems to be related to the large portion of TiB_2 which causes poor sinterability and agglomation of the particles. The values of microhardness and fracture toughness were determined by following equation (3) of Vicker's indentation method and the formula (4) proposed by Lawn and Fuller.[21]

$$H_V = 1.854 \frac{F}{D^2} \tag{3}$$

where, H_v : Vicker's hardness (kgf/mm^2)
F : load (kg)
D : diamond indentor (mm)

$$K_{IC} = \frac{1}{\pi^{1/2}\tan\theta} \cdot \frac{P}{C^{3/2}} \tag{4}$$

K_{IC} : fracture toughness (MPa · m$^{1/2}$)
P : load (kg)
C : half crack (μm)

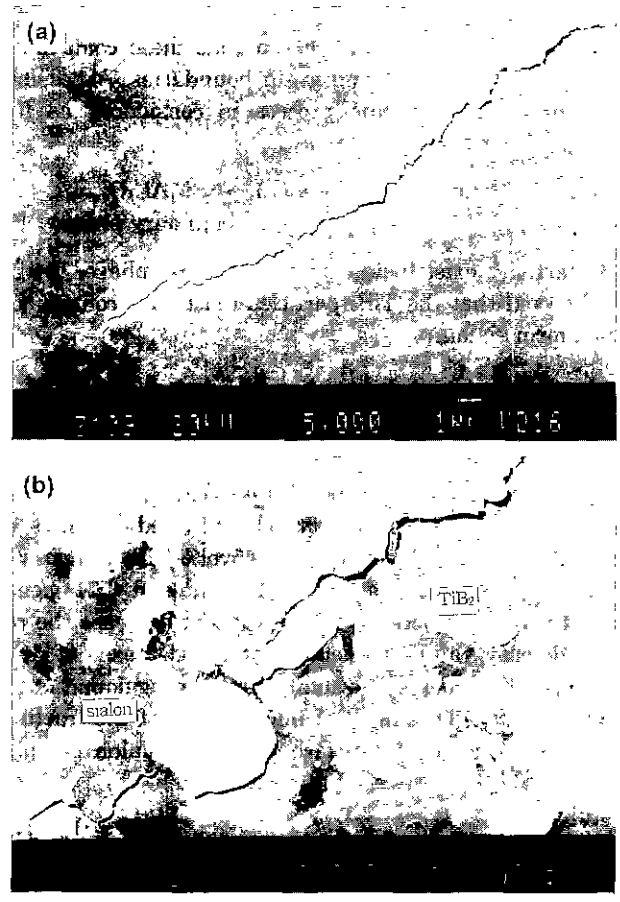

Fig. 6. (a) Crack propagation in a monolithic sialon sample (b) Crack deflection in sialon-30 vol.% TiB_2 composite.

θ : 68°

The microhardness decreased with increasing the TiB_2 content. To investigate the interaction between the propagating crack and the specific microstructural features, several indentations were applied on the etched surfaces. The fracture behaviour of the monolithic sialon showed the mixed transgranular and intergranular fracture. Fig. 6(a) in which the crack mainly propagates along the sialon grains or partially deflects the elongated lod-like grains. The fracture toughness increased with TiB_2 content to a maximum at 30 vol.% composites and then decreased. It can be supposed that the crack propagates the agglomation of TiB_2 particles without deflection. The toughness value of 30 vol.% composite was 22% higher (7.1 MPa · m$^{1/2}$) than that of monolithic sialon. The composit containing 30 vol.% TiB_2 (Fig. 6b) showed crack deflection around the TiB_2 particles that can result in improvement of fracture toughness.[6-7,19-20] The amount of crack deflection out of plane increased with increasing TiB_2 particle content.

4. Electrical properties and electrical discharge machining(EDM)

In the Table 3 were given the average values of electr-

Table 3. Electrical Resistivities of Sialon-TiB_2 Composites

Sample \ Resistivity	Electrical resistivity ($\Omega \cdot cm$)	Sheet resistivity ($\Omega \cdot cm$)
Sialon	range error	range error
Sialon-15 vol.% TiB_2	range error	range error
Sialon-30 vol.% TiB_2	1.2×10^{-4}	0.767932
Sialon-45 vol.% TiB_2	1.0×10^{-6}	0.00454

ical resistivities. The electrical resistivities of the monolithic sialon and composite containing 15 vol.% TiB_2 were so high that they could not be measured. The composites added 30 vol.% and 45 vol.% TiB_2 had the electrical resistivities of 1.2×10^{-4} $\Omega \cdot cm$ and $1.0\times10^{-6}\Omega \cdot cm$, respectively. It has been reported that the electrical conductivity of composite is effected by the amounts and chain formation, which is therefore linked to size and distribution of electro conductive particles.[14] Among these factors are size and distribution of particle important. Even if the added amounts are few, the composites can be good conductor, when the fine particles are homogeneously dispersed in a matrix. In view of the results of electrical resistivity achieved, the composites containing more than 30 vol.% TiB_2 make electrical discharge machining possible. The fundamental principle of EDM is the thermal erosion of materials as a result of a spark discharge between the tool and workpiece which are connected to two electrodes. There is a relationship among a EDM machining rate (W), surface roughness (Ra), spark current peak (Ip) and pulse interval (τ_{on}) as follows;[21]

$$W \approx \tau_{on} \times I_p$$
$$R_a \approx \tau_{on} \times I_p \quad (5)$$

Since machining rate and surface roughness are dependent upon the peak current and pulse interval, longer pulse interval and larger peak current cause shorter machining time because of faster machining rate, however, poorer surface roughness becomes because of greater machining roughness.[12-13,18] Accordingly, it is important to establish a releverant operating condition between machining rate and surface roughness. The material with the resistance of larger than 10 $\Omega \cdot cm$ can be machined by EDM. A monolithic sialon and a sialon-15 vol% TiB_2 composite have too large electrical resistances to be machined by EDM and evaluated their resistance. The machining rate was increased with the addition of titanium boride up to 45 vol.% and decreased after showing the maximum value. This behavior may be related to the reduced machining rate due to the inhomogeneous distribution of titanium boride in the composite specimen which causes insufficient electric field between an electrode and the specimen. These supported the observations of surface roughness. The surface roughness after adding 30 vol.% and 45 vol.% TiB_2 are 9.8 and 10.7 μm, respectively. The cutting velocities and maximum surface roughness for sialon-30 vol.% and 45 vol.% of TiB_2 prepared by wire EDM were 1.6 mm/min, 9.8 μm, 1.3~1.9 mm/min and 10.7 μm, respectively. The sinking velocities and maximum surface roughness for these composites prepared by die-sink EDM were 0.06 mm/min and 19.5 μm after the first machining, and 1.2 mm/min and 6.2 μm after the second process, respectively. Fig. 7(a,b) are SEM images of the machined surfaces. These photos show debris with lump shape. Considering the composition of raw materials and thermodynamical equilibria among them, the debris seem to be titanium oxides and silicon oxide formed by melting and solidification of particles at a high temperature during EDM process. The weak peaks of TiO_2 and SiO_2 could be detected in the X-ray diffraction pattern. Fig. 7(b) also shows voids and microcracks. The voids and microcracks may be formed by the defection of titanium boride particles and the thermal shocks during EDM, respectively. These cracks are believed to promote the EDM process itself. The surface roughness can be improved by the second and the third machining. Hence, the machinability of a composite material depends on amount of additives, size distribution of conductive materials and uniform distribution of the particles. In this study, a composite material

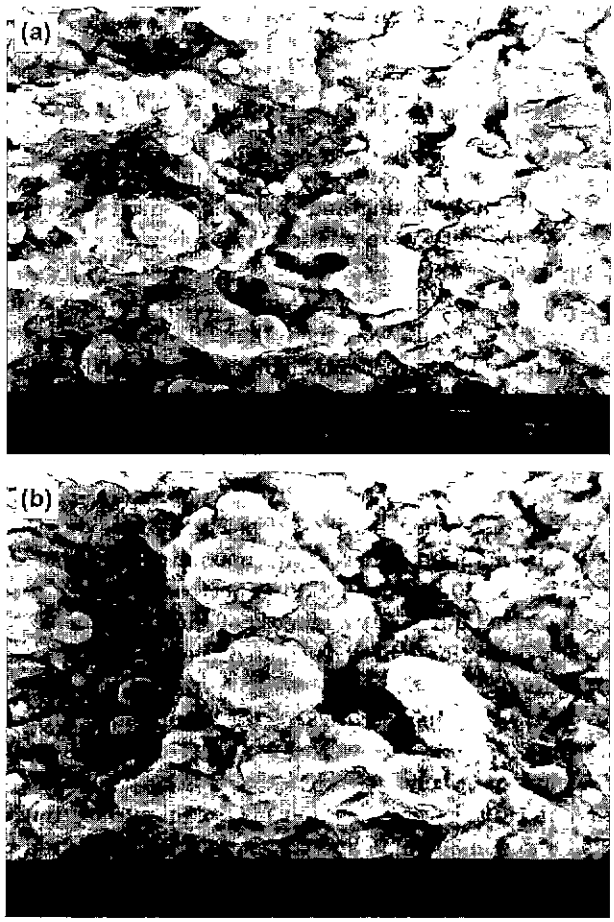

Fig. 7. SEM micrographs of sialon-30 vol.% TiB_2 composite after EDM.

with 30 vol.% of titanium boride inside has superior performance.

IV. Conclusions

Sialon composites with various amount of TiB_2 were fabricated by hot pressing and their mechanical properties and machinability were studied. The followings were obtained in this study:

1. Sintered densities of monolithic sialon and the sialon with 15~30 vol% TiB_2 were more than 99% relative density, respectively, however, the sialon with 45% TiB_2 had more than 98% relative density.

2. The flexural strength of the composites increased with TiB_2 content, however, that of the composites with 45 vol.% was lower than the strength of sialon. TiB_2 addition decreased their hardness. Their toughness increased with TiB_2 addition, showed the maximum value of 7.1 $MPa \cdot m^{1/2}$ at 30 vol% of TiB_2 and decreased with further addition. The enhanced toughness of composites was due to crack deflection which dissipated the energy for crack propagation.

3. Electrical conductivities of the composites with 30 vol.% and 45 vol.% TiB_2 were 1.2×10^{-4} $\Omega\cdot$cm and 1.0×10-6 $\Omega\cdot$cm, respectively.

4. The cutting velocities and maximum surface roughness for sialon-30 vol.% and 45 vol.% of TiB_2 prepared by wire EDM were 1.6 mm/min, 9.8 μm, 1.3~1.9 mm/min and 10.7 μm, respectively. The sinking velocities and maximum surface roughness for there composites prepared by die-sink EDM were 0.06 mm/min and 19.5 μm after the first machining, and 0.2 mm/min and 6.2 μm, after the second process, respectively.

5. Electrical discharge machining mechanism related to melting and evaporation of the materials. Considering the composition of raw materials and thermodynamical equilibria, the debris with lump shape on the machined surface seems to be formed by the resolidification of titanium and silicon oxides at a high temperature during EDM process.

Acknowledgment

This work was supported by GRANT No. 971-0801-007-1 from the Korea Science and Engineering Foundation.

References

1. M. Mitomo et. al, "The Formation of Single Phase Si-Al-O-N-Ceramics," *Yogyo-Kyokai-Shi*, **86**(11), 526-531 (1978).
2. T. Eustrom and M. Nygren "Sialon Ceramics," *J. Am. Ceram. Soc.*, **75**(2), 259-276 (1992).
3. Siddharta Bandyopadhyay et al, "Densification Behavior and Properties of Y_2O_3-Containing α-Sialon-Based Composites," *J. Am. Ceram. Soc.*, **79**(6), 1537-1545 (1996).
4. K. H. Jack, "Sialon: A Study in Materials Development, Non-oxide Technical and Engineering Ceramics," "Non-Oxide Technical and Engineering Ceramics," pp. 1-30, *Elsevier Applied Science*, London, 1986.
5. T. Ekstrom, N. Ingelstrom, "Characterisation and Properties of Sialon Materials," Ibid 231-54 (1986).
6. G. C. Wei and P. F. Becher, "Improvements in Mechanical Porperties in SiC by Addition of TiC Particles," *J. Am. Ceram. Soc.*, **67**(8), 571-574 (1984).
7. Carl H. McMurty, Wolfgang D. G. Boecker, Srinivasa G. Seshadri, Joseph S. Zanghi, and John E. Garnier, "Microstructure and Material Properties of SiC-TiB_2 Particulate Composites," *Am. Ceram. Soc. Bull.*, **66**(2), 325-329 (1987).
8. Bor-Wen LIN and Takayoshi ISEKI, "Effect of Thermal Residual Stress on Mechanical Properties SiC/TiC Composites," *Br. Ceram. Trans. J.*, **91**, 1-5 (1992).
9. R. P. Wahiand B. Ilschner, "Fracture Behaviour of Composites Based of Al_2O_3-TiC," *J. Mater. Sci.*, **15**, 875-85 (1980).
10. Ken Takahashi, Ryutarou Jimbou, Yasuo Matsuhiya and Tetsus Kosugi, "Electrical Resistivity of SiC-ZrB_2 Electroconductive Ceramic Composites," *Yogyo-Kyokai-Shi*, **94**(1), 214-218 (1986).
11. N. F. Petrofes and A. M. Gadalla, "Electrical Discharge Machining of Advanced Ceramics," *Am. Ceram. Soc. Bull.*, **67**(6), 1048-1052 (1988).
12. M. Ramulu, "EDM Sinker Cutting of a Ceramic Particulate Composite, SiC-TiB_2," *Advanced Ceram. Mat.*, **3**(4), 324-327 (1988).
13. Eiji Kamijo, Masaaki Honda et. al, "Electrical Discharge Machinable Si_3N_4 Ceramics," *Sumitomo Electric Technical Review*, **24**, 183-190 (1985).
14. A. Bellose, S. Guicciardi and A. Tampieri, "Development and Characterization of Electroconductive Si_3N_4-TiN Composites," *J. Europ. Ceram. Soc.*, **9**, 83-93 (1992).
15. Martin, C., Mathieu, P. & Cales, B., Electrical Discharge Machinable Ceramic Composite. *Mater. Sci Eng.*, **A109**, 351-356 (1989).
16. Tokura, H., Kodoh, I., & Yoshikawa, H., Ceramic Material Processing by Electrical Discharge in Electrolyte, *J. Mater. Sci.*, **24**, 981-998 (1989).
17. Mamulu, M. Taya., EDM Machinability of SiCw/Al Composites, *J. Mater. Sci.*, **24**, 1103-1108 (1989)
18. A. M. Gadalla, "Electrical Discharge Machining of Advanced Materials," Processing and Fabrication or Advanced Materials for High Temperature Applications. pp. 193-209, A Publication of TMS, Ohio, 1992.
19. T. Mah, M. G. Mendiratta, and H. A. Lipsitt, "Fracture Toughness and Strength of Si3N4-TiC Composites," *Am. Ceram. Soc. Bull.*, **60**(11), 1229-1240 (1981).
20. Y. K. Park, "Mechanial and Electrical Properties of Hot-Pressed Silicon Carbide-Titanium Carbide Composites," *J. Kor. Ceram. Soc.*, **32**(10), 1194-1202 (1995).
21. B. R. Lawn & E. R. Fuller, "Equilibrium Penny-Like Crack in Indentation Fracture," *J. Mater. Sci.*, **10**(12), 2016-2024 (1976).
22. Je-ku Yoo, "Electrical Discharge Machining," pp. 1-299, TaeKwangSeorim, Scoul, 1992.